Elastic Liquid Jet Impaction on a High-Speed Moving Surface

B. Keshavarz and S. I. Green
Dept. of Mechanical Engineering, University of British Columbia, Vancouver, BC, V6T 1Z4, Canada

D. T. Eadie
Kelsan Technologies Corporation, 1140 West 15th Street, North Vancouver, BC, V7P 1M9, Canada

DOI 10.1002/aic.13737
Published online January 31, 2012 in Wiley Online Library (wileyonlinelibrary.com).

In the railroad industry a friction-modifying non-Newtonian liquid, showing elastic behavior, may be applied to the rail in the form of a liquid jet. The interaction of this elastic liquid jet and the moving surface—specifically whether it splashes or adheres without splash—is important in this industrial application. Twelve different elastic liquids with widely varying relaxation times were tested to isolate the effect of elasticity from other fluid properties. Using high-speed imaging, the interaction between the impinging jet and the moving surface could be captured and analyzed. Although similar to Newtonian jets, for which the Reynolds number plays a major role, the Deborah number was also salient to the splash of elastic liquids. At the elevated Weber numbers of the testing, the Weber number had a much smaller impact on splash than did the Reynolds or Deborah numbers. The ratio of the surface velocity to the jet velocity has only a small effect on the splash. © 2012 American Institute of Chemical Engineers *AIChE J*, 58: 3568–3577, 2012
Keywords: jet impaction, splash, deposition, elasticity, impingement, moving surface

Introduction

The impingement of a non-Newtonian liquid jet on a moving dry substrate is important in a number of industrial applications. Spray-coating and polymer impingement cooling are good examples of such industrial applications. Another such application is liquid friction modifier (LFM) coating of the railroad track top of rail. The LFM that has been studied by the authors is a water-based suspension of polymers and inorganic solids showing non-Newtonian behavior.[1] This liquid is usually applied on the top surface of the rail through sprayers mounted on rail cars, locomotives, or track maintenance vehicles.[2] Reduced fuel consumption, reduced rail/wheel wear, and decreased lateral (curving) forces are some of the benefits of LFM utilization.

In current practice in the railroad industry, air-blast atomizers transfer the LFM (atomized to form ligaments and droplets) to the rail surface. Major issues in this application are the impaction of the liquid on the surface, and the interaction between the particles and cross-flowing air.[3] For effective deposition on the rail, the droplets/ligaments should have sufficient velocity to avoid excessive deflection in the crosswind but not have such a high velocity as to cause splash or rebound after impaction. Both excessive deflection and splash would cause an undesirable reduction of transfer efficiency.[4,5]

There are many studies in the literature of Newtonian droplet impact on a dry/wet stationary surface. Research done by Rein,[6] Rioboo et al.,[7] Yarin,[8] and Deegan et al.[9] are good examples in this area. These authors have studied the effects of fluid properties such as viscosity, density, and surface tension on the postimpact outcomes. The impact of a single droplet on a dry surface was classified by Rein[6] into three types: deposition or spreading, splash, and bouncing. Rioboo et al.[7] later expanded this classification to six possible outcomes: deposition, prompt splash, corona splash, receding breakup, partial rebound, and complete rebound. Range and Feuillebois[10] and Crooks and Boger[11] have studied more specifically the effects of surface roughness on the impaction outcome and have shown that surface roughness decreases the splash threshold significantly. More detailed results about Newtonian droplet impact on a dry solid stationary surface can be found in recent reviews by Yarin[8] and Deegan et al.[9]

The impact of a droplet on a moving surface is also of interest in many industrial applications. Mundo et al.[12] studied the impact of a Newtonian droplet on a moving substrate and concluded that the tangential velocity of the droplet, in the frame of reference of the solid substrate, is less important than the normal component of droplet speed. In contradiction to their finding, several authors (e.g., Povarov et al.,[13] Courbin et al.,[14] Okawa et al.,[15] and Fathi et al.[16]) have reported that the tangential speed plays a significant role and include it in their splash/deposition criteria. Povarov et al.[13] studied the case of impact on a spinning disc. They observed that the air boundary layer, caused by the tangential velocity of the disc, lifts the droplet from the surface. Courbin et al.[14] and Bird et al.[17] found that asymmetric splashes occur on impaction of a droplet on a moving dry surface; in the frame of reference of the moving dry surface, the splash is strengthened in the downstream tangential direction of the impacting droplet and weakened in the upstream direction. In recent work, Bird et al.[17] suggest a new physical model for the impact of a droplet on a moving surface. Their model highlights the interaction between the after-impact lamella and the moving surface.[17,18]

Correspondence concerning this article should be addressed to S. I. Green at green@mech.ubc.ca or sheldon.green@ubc.ca.

The widespread use of non-Newtonian liquids in industry has motivated many recent works studying the impact of a non-Newtonian droplet on a stationary/moving surface. Special attention has been paid to the behavior of elastic liquids. Bergeron et al.,[19] Crooks and Boger,[11] Roux et al.,[20] and Dressler et al.[3] report that elasticity helps in controlling the droplet deposition and inhibits the splash. Bergeron et al.[19] showed in their experiments with polyethylene oxide (PEO) solutions that the high elongational viscosity of elastic liquids helped dampen the droplet's spreading after impact, preventing splash/rebound.

Recent experiments by Dressler[21] suggested that air-blast atomizers are less than ideal in transferring LFM to the rail top surface. The high-speed atomizing air jet carried away some of the droplets/ligaments from the impacting surface, which leads to a lower transfer efficiency. To reduce this effect, a simple new airless, nonatomizing sprayer was developed by the authors. This sprayer produces a high-speed liquid jet that under some conditions does not break up. In contrast to the large amount of research done in the area of droplet impact on stationary/moving substrates, we know of only a few studies of a high-speed Newtonian or non-Newtonian liquid jet impinging on a high-speed moving substrate.

Liu and Lienhard[22] studied the interaction of a Newtonian liquid jet and a stationary substrate but were mainly concerned with heat transfer. A mathematical model has been proposed by Hlod et al.[23] to describe the interaction of a low-speed highly viscous Newtonian jet with a slow moving surface. As the speeds in their work were low, splash is not mentioned in their model. In recent work, Keshavarz et al.[24] have studied the impact of a Newtonian jet on a moving rail surface. They found that, in contrast with the droplet case, in jet impingement viscous effects are more important in determining splash than is surface tension. This means that the main splash criterion was jet Reynolds number, not the Weber number. If the jet Reynolds number is defined based on the jet velocity in the frame of reference of the solid substrate, then the authors have shown that the jet impaction angle plays a negligible role on splash. They also showed that surface roughness dramatically impairs splash. Finally, for the high Weber numbers (>200) used in their experiments, they found that Weber number does not affect splash. The criterion for splash of droplets proposed by Bird et al.[17] was redefined for the jet impact of a Newtonian liquid on moving targets. They showed that the simple model predicts the main experimental results for Newtonian jets.

For the impingement of a Newtonian, noncavitating liquid jet on a moving surface, the splash threshold is a function of the relative jet speed,* (V_{rel}), the jet diameter, (D), the impingement angle in the frame of reference of the surface, (α), the fluid density, viscosity, and surface tension, (ρ, μ, σ), and the surface roughness,[24] (ε).† These seven variables are reduced to four dimensionless groups

$$Re = \frac{\rho V_{rel} D}{\mu} \tag{1}$$

$$We = \frac{\rho {V_{rel}}^2 D}{\sigma} \tag{2}$$

*The relative jet speed is the magnitude of the vector sum of the jet velocity, V_j, and the surface velocity, V_S, that is, $V_{rel} = \sqrt{V_j^2 + V_s^2}$ (Figure 4).

†It may also be a function of the surface material (e.g., as represented by the contact angle of a droplet on the surface), and the ambient air properties but these effects are not considered here.

Table 1. Elastic Liquids Tested

	Longest Relaxation Time (from CaBER) (ms)	Longest Relaxation Time (from Rouse-Zimm Theory) (ms)	Shear Viscosity (Pa·s)
8000K PEO-0.5 wt %	101.6	94.00	0.026
8000K PEO-0.1 wt %	29.8	47	0.009
4000K PEO-0.5 wt %	39	28.3	0.017
4000K PEO-0.25 wt %	23.6	18.30	0.011
4000K PEO-0.075 wt %	4.9	11.64	0.007
4000K PEO-0.1 wt %	6.3	9.98	0.006
1000K PEO-1 wt %	Not accurate	6.4	0.038
1000K PEO-0.5 wt %	Not accurate	1.7	0.01
300K PEO-1 wt %	Not accurate	0.21	0.009
300K PEO-0.5 wt %	Not accurate	0.17	0.007
100K PEO-1 wt %	Not accurate	0.028	0.007
100K PEO-0.5 wt %	Not accurate	0.026	0.007

$$\alpha : \text{Impingement angle in the frame of reference of the surface} \tag{3}$$

$$\frac{\varepsilon}{D} : \text{Relative roughness} \tag{4}$$

For the elastic liquids, another variable will be added to our previous seven parameters. This new variable is the longest relaxation time, λ, of the PEO solution, which is a measure of its elasticity. This means that for the elastic liquids another dimensionless group including λ should be added. A widely used dimensionless parameter containing λ is the Deborah number

$$De = \frac{\lambda V_{rel}}{D} \tag{5}$$

Splash of an elastic liquid should be a function of five dimensionless parameters: Re, We, α, $\frac{\varepsilon}{D}$, and De.

The authors could find no previous literature on the interaction of an elastic liquid jet with a moving surface. This article builds on the previous work by exploring the effects of elasticity on liquid jet impaction on a moving surface.

Materials and Methods

Twelve different solutions of water and PEO were used as the elastic test liquids, to study the effects of elongational viscosity (Table 1). The solution shear viscosity and longest relaxation time were, respectively, measured by a HAAKE VT550 viscometer and a HAAKE CaBER 1 extensional rheometer at a temperature of 25°C. Figures 1 and 2 show two typical measurements from shear (HAAKE®) and extensional (CaBER®) rheometers, respectively. Dilute PEO solutions showed a slight shear thinning behavior at low shear rates and then reached a constant viscosity close to the solvent viscosity at high shear rates (Figure 1). As the values of shear rate inside the nozzle and at the moment of jet impact are very high, the value of high-shear rate viscosity (η_∞) is reported as the fluid viscosity. For solutions with low elasticity (PEO solutions with lower molecular weights or concentrations), readings from the extensional rheometer were not accurate or repeatable. This is a well-known challenge for measurements of relaxation times related to low viscosity dilute polymeric solutions, which is discussed in detail by Rodd et al.[25] The main challenge is that the liquid bridge in

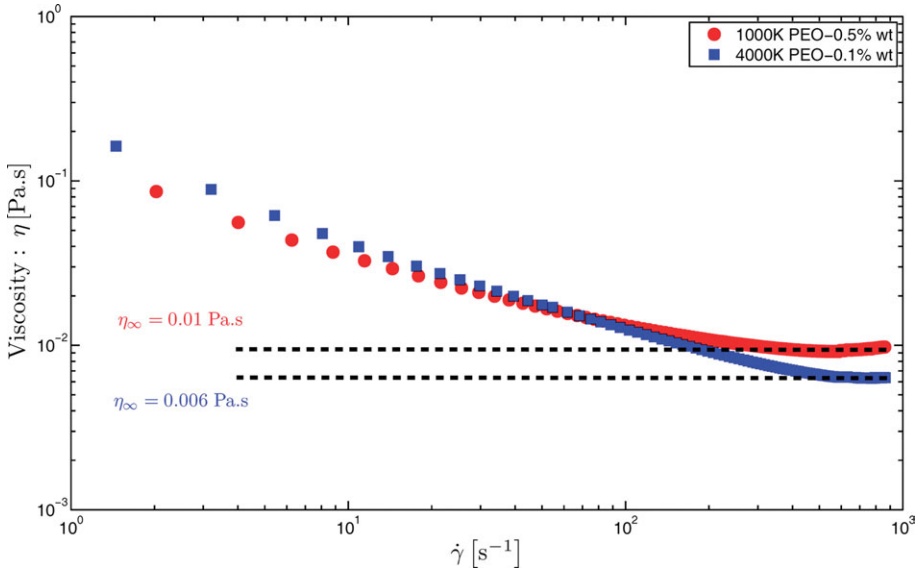

Figure 1. Viscosity measurements for two sample PEO solutions.

[Color figure can be viewed in the online issue, which is available at wileyonlinelibrary.com.]

the CaBER® is not elastic or viscous enough and it breaks up before the plates are separated (i.e., before the start of diameter recordings). Hence, Rouse–Zimm theory (Doi and Edwards[26]) was used to calculate the longest relaxation times in those cases. Once the fluid was elastic enough and liquid filament lived well more than plate's separation time, measurements were possible (Figure 2). As discussed by Rodd et al.,[25] an elastocapillary region can be found in the evolution of the liquid filament diameter, which arises from a balance between capillary force and the elastic resistance of polymer; its signature is an exponential thinning of diameter with time from which the relaxation time can be deduced. The relaxation time, which is a measure of elasticity, varied by four orders of magnitude for the PEO mixtures.

The fluid surface tensions were measured by a Du Noűy ring apparatus at a temperature of 25°C; all surface tension values were within ±5% of that of water (72.1 mN/m).

To generate the liquid jet, an accumulator was first filled with the elastic liquid. The accumulator is connected to a valve and a nozzle with an internal diameter of 648 μm. The accumulator is pressurized with nitrogen gas and a high-speed liquid jet was created at the nozzle exit when the valve was opened. This jet impacted on a fast moving projectile. The projectile had a 13-mm thick polished steel surface (the top surface of an AREMA 136# rail) fastened to a wooden base carrier (Figure 3). To study the effect of surface roughness on impaction, sandpaper with a roughness height to jet diameter ratio of 0.1 was selected and attached to part of the top surface of the projectile.

The driving force for the projectile was an air cannon, which was designed and built for experiments done by Dressler.[21] After firing the projectile leaves the air cannon barrel and passes beneath the spraying nozzle. An energy dissipation device then stops the projectile (Figure 4). The

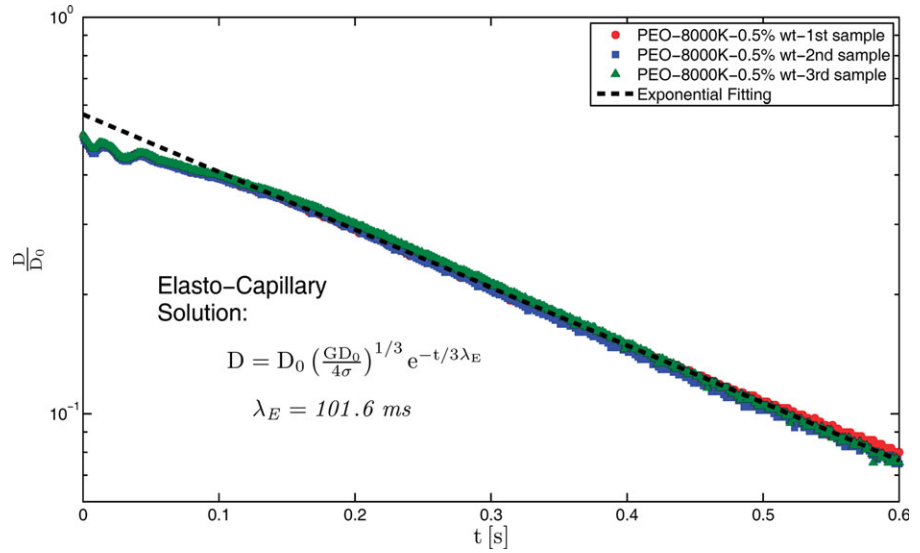

Figure 2. Measurement of relaxation time for 8000K-PEO solution using data from CaBER®.

[Color figure can be viewed in the online issue, which is available at wileyonlinelibrary.com.]

Figure 3. Projectile.

[Color figure can be viewed in the online issue, which is available at wileyonlinelibrary.com.]

projectile speed could be varied from less than 1 m/s to 25 m/s by changing the air cannon air pressure. This test setup allowed us to vary the surface speed independent of jet velocity, and also guaranteed that impingement occurs on a dry moving surface, which is a good representation of the rail surface coating process. Figure 5 illustrates the geometry of jet impingement.

For high-speed imaging, a Phantom V12 high-speed video camera along with a high-intensity halogen lamp for backlighting were used (Figure 6), enabling the visualization of jet impingement on the fast moving projectile. Resolution of the camera and its frame rate were, respectively, set as 800 $\times$ 1200 pixels and 6200 pictures per second; the exposure time was set at 9 μs.

The projectile speed could be easily measured by analysis of high-speed captured images. Separate sets of high-speed magnified images of the jet at different heights from the nozzle exit were captured for jet diameter measurements. They were analyzed by an image processing code written in MatLab®. Mass flow rate measurements of the discharged liquids were also done by weighing the liquid discharged from the nozzle over a span of 30 s, then the average jet velocities were obtained by dividing the mass flow rate by the fluid density and jet cross-sectional area.

Results and Discussion

Flow rates through the nozzle

To find the jet velocity, flow rate measurements were completed for all twelve different PEO solutions. The flow of these elastic solutions through a circular nozzle is significantly different from the flow of simple Newtonian liquids. The latter case has been studied thoroughly in Lefebvre[27] and Keshavarz et al.[24] Two dimensionless groups can express the single-phase Newtonian liquid discharge from a nozzle: Reynolds number and discharge coefficient, which is defined as

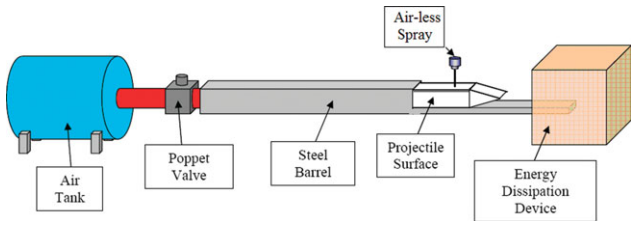

Figure 4. Experimental setup: linear transverse system.[21]

[Color figure can be viewed in the online issue, which is available at wileyonlinelibrary.com.]

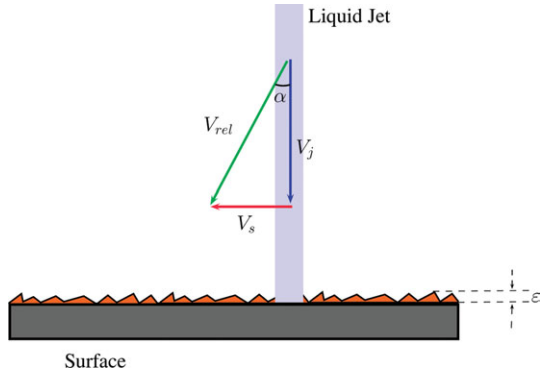

Figure 5. Jet pathline angle in frame of reference of moving surface.

[Color figure can be viewed in the online issue, which is available at wileyonlinelibrary.com.]

Discharge Coefficient:

$$C_d = \frac{\text{Actual Mass Flow Rate}}{\text{Ideal Mass Flow Rate}} = \frac{\dot{m}}{A_n\sqrt{2\rho.\Delta P}} \quad (6)$$

However, this common approach cannot be replicated for the discharge flow of elastic liquids, as it neglects the elongational forces that are present in the flow (Boger[28] and Boger and Walters[29]). Elongational forces can be considered, for example, as proposed by Boger[28] and Rothstein and McKinley,[30] by introducing other dimensionless numbers such as the Deborah number or the Elasticity number. The latter is defined to be the Deborah number over the Reynolds number

$$El = \frac{De}{Re} \quad (7)$$

As mentioned by other researchers (Boger[28] and Rothstein and McKinley[30]), even considering the Deborah or Elasticity number effects does not completely explain elastic fluid behavior at high Reynolds numbers. Consequently, most work has focused on very low Reynolds number flow (creeping flow) through nozzles/orifices (Rothstein and McKinley[30] and Cartalos et al.[31]).

To analyze the flow rate data from the current experiments with PEO solutions, we attempted the same approach used

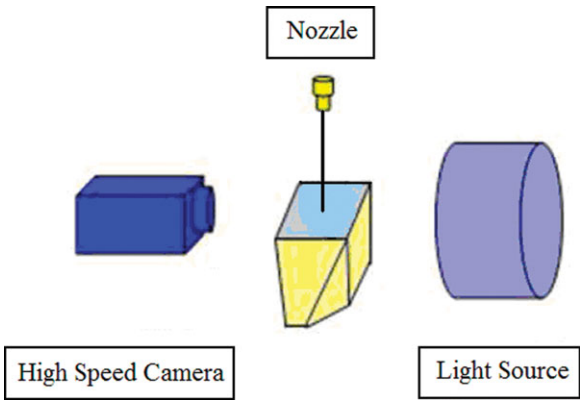

Figure 6. High-speed camera and light source position relative to the projectile and the nozzle.

[Color figure can be viewed in the online issue, which is available at wileyonlinelibrary.com.]

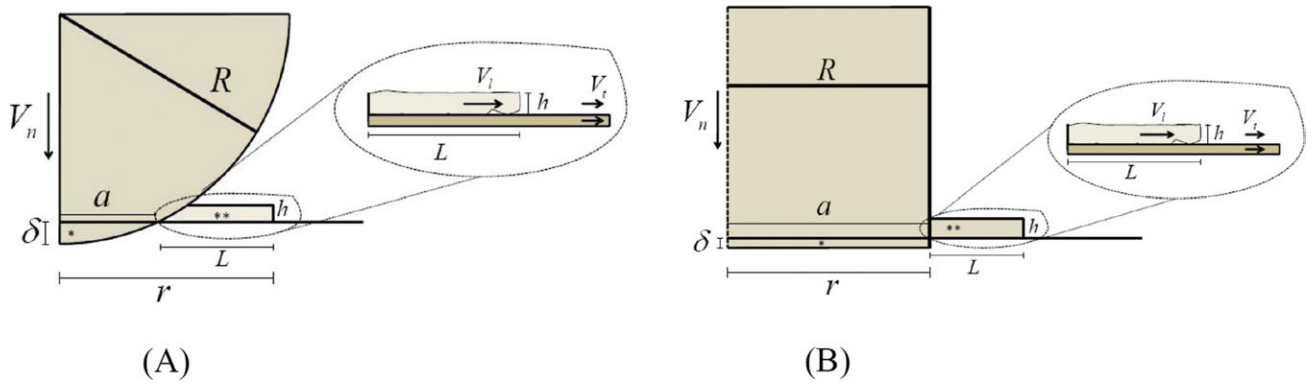

Figure 7. (A) Schematic of the model used for drop impact.[17] (B) Schematic of the model used for jet impact.[24]

[Color figure can be viewed in the online issue, which is available at wileyonlinelibrary.com.]

in related works (Boger,[28] Rothstein and McKinley,[30] and Cartalos et al.[31]); however, those studies were limited to the creeping flow regime. No robust conclusions could be made in our case for all different molecular weights and concentrations. We believe that the data do not collapse straightforwardly owing to the nonlinearity of both inertial and elastic forces at the high *Re* and *De* in the nozzle.

In this work, the flow rate at a certain driving pressure difference across the nozzle was measured. From these data, and knowing the values of fluid viscosity and relaxation time from rheometry, one can easily calculate Reynolds, Deborah, and Elasticity numbers at a certain pressure difference. For other experiments, only interpolation of the flow rate data was required for calculating the jet velocity and other variables.

Splash/nonsplash results

Figure 8 shows two photos of elastic liquid jet impaction. Figure 9 shows an equivalent pair of photos of Newtonian liquid jet impaction. For equal values of shear viscosity, adding elasticity led to significant improvements of the splash threshold in all the tested cases. Elastic/elongational forces were helpful in preventing splash as they increased the resistance of the moving lamella to lift off and kept it attached to the moving surface even at high impaction speeds (see, for example, part A of Figure 8). When splash does occur, the splash of elastic liquids differed from Newtonian liquid splash. For example, a comparison of Figure 8B with Figure 9B shows that due to increased elasticity postimpact elastic droplets are much larger than postimpact Newtonian ones. Furthermore, in the elastic liquid cases thin films or ligaments connect the droplets together; these filaments do not exist in the Newtonian splash cases. Similar findings were reported about atomized droplet sizes for elastic liquids in Li et al.[1] and postimpact droplet sizes in the case of elastic droplet impact on a moving surface by Dressler et al.[3]

Figures 10 and 11 show the splash/nonsplash data for elastic liquid jet impaction on smooth and rough surfaces in terms of Deborah and Reynolds numbers. In both graphs, the line separating splash from deposition has a positive slope: 0.13 for the smooth surface and 0.081 for the rough one.[‡] The positive slope of the separation line means that increasing the Deborah number causes the critical Reynolds number for splash to also increase. In other words, adding elasticity to the liquid jet helps to avoid splash, which is in accordance with similar work done on droplet impact (Bergeron et al.,[19] Crooks and Boger[11] Roux et al.,[20] and Dressler et al.[3]).

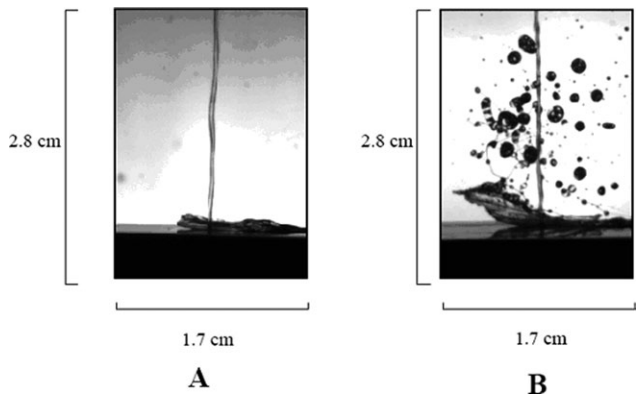

Figure 8. Projectile is traveling from left to right with a velocity equal to 5.9 m/s in both (A) and (B).

The elastic liquid jet velocity is 20.3 m/s in (A) and 30.0 m/s in (B).

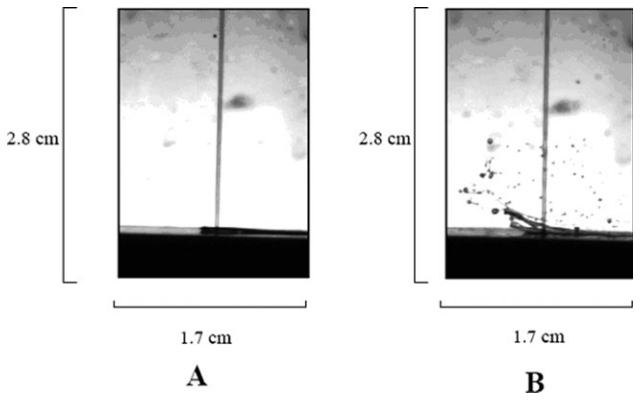

Figure 9. Projectile is traveling from left to right with a velocity equal to 3.6 m/s in both (A) and (B).

The Newtonian liquid jet velocity is 12.5 m/s in (A) and 18.6 m/s in (B).

[‡]The dependence of the slope of the dividing line on roughness ratio will be considered in follow-on work.

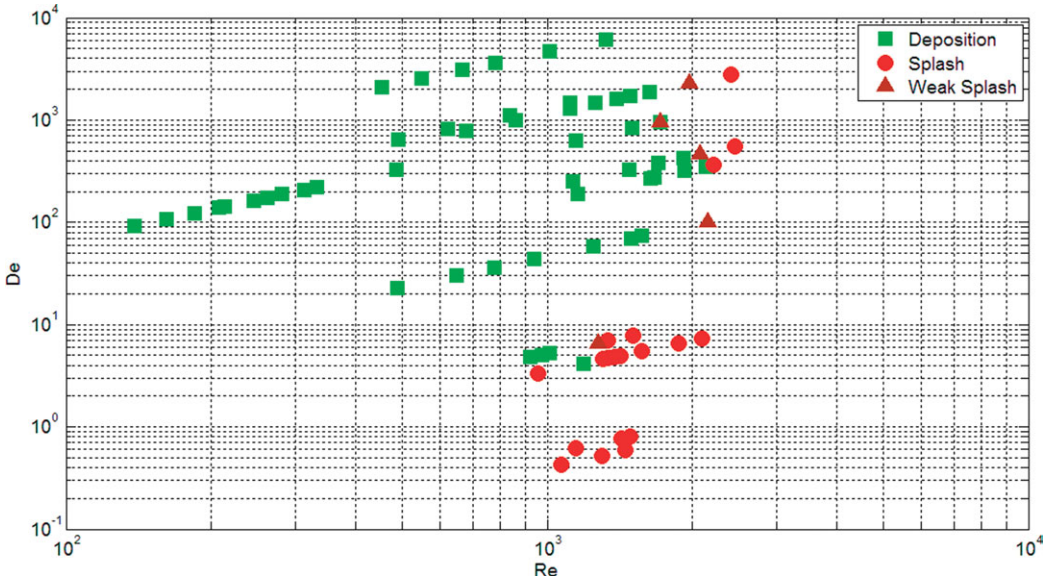

Figure 10. Splash/non-Splash boundary for elastic liquids impacting on the smooth surface.

[Color figure can be viewed in the online issue, which is available at wileyonlinelibrary.com.]

The fact that Reynolds and Deborah numbers are the primary determinants of liquid splash motivated the authors to extend our simple model for Newtonian jet impact[24] to the case of elastic liquids. What follows is a brief description of the previous model and the way elastic effects will be introduced in the model. Then, there will be a comparison of the model predictions with experimental data.

The model proposed by Keshavarz et al.[24] is based mainly on the original modeling of drop impact on moving surfaces done by Bird et al.[17] Figure 7A shows a schematic model for spherical droplet impact on a moving substrate. The lamella is the portion of the drop that has contacted the solid line (region*) and is transferred into an outward moving film with thickness h and length L. The normal speeds of the droplet, tangential speed of the surface and the lamella are, respectively, V_n, V_t, and V_l. The relative kinetic energy will be $\rho(V_l - V_t)^2L^2h$ and the surface energy will scale as σhL. According to Bird et al.,[17] splash occurs when the relative kinetic energy of the lamella is much greater than the surface energy or in other words when the surface energy is not big enough to suppress the kinetic energy

$$\frac{\rho(V_l - V_t)^2 L}{\sigma} \geq C \approx 1 \tag{8}$$

where the constant value of C is a function of surface and air properties.[§] This criterion also explains the occurrence of the asymmetric splash observed by Courbin et al.[14] Keshavarz et al.[24] start from the same criterion and apply it to a different geometry for jet impact, that is, an axisymmetric column of liquid impacting on a moving substrate (Figure 7B). To simplify and relate this criterion to the main dimensionless numbers, (i.e., Re, We, and relative angle or velocity ratio) several assumptions were made in the Bird et al.[17] modeling that are repeated in the Keshavarz et al.[24] work:

1. Conservation of mass dictates that the volume of droplet in* and ** regions are equal to each other.

2. The thickness of the propagating lamella is proportional to the momentum boundary layer thickness in the liquid, that is, $h = c_1\sqrt{vt}$, where c_1 is a constant of order 1. The aforementioned assumption is widely used in modeling lamella thickness behavior; however, recent experiments by Ruiter et al.[18] have shown that the lamella thickness is a much more complex function of different parameters such as viscosity, time, droplet velocity, roughness, and so on. It is of course expected that for the splashing of an elastic liquid droplet, the extensional properties of the fluid should also affect the lamella thickness.

3. The critical time at which splash starts, t_c, corresponds to the moment at which the lamella distinctively separates from the drop. This criterion leads to the approximation $L(t_c) \approx a(t_c)$.

Their criterion for droplet splash on moving substrates can be easily simplified and re-expressed in terms of dimensionless numbers based on the relative velocity ($V_{rel.} = \sqrt{V_n^2 + V_t^2}$) as

$$We.Re^2\left[\frac{1}{6} - \left(\frac{\sin^2\alpha}{6} + \frac{\sin\alpha}{Re}\right)\right]^2 \geq K \tag{9}$$

where $We = \frac{\rho V_{rel.}^2 R}{\sigma}$, $Re = \frac{V_{rel.}R}{\nu}$, and α is $arc\tan\left(\frac{V_t}{V_n}\right)$. Here, α is the angle relative to the surface normal direction, in the frame of reference of the surface, made by a fluid pathline (Figure 5). The predictions of this simple model for Newtonian jet impact agreed qualitatively with experimental results. In the range of tested jet/substrate speeds, both the model and experiments showed higher effects of Reynolds number on splash than Weber number or jet angle.[24]

For elastic liquid jets, the same general approach can be taken to build a simple model. Physically, elongational deformation in the lamella will result in locally high extensional viscosity, which will in turn change the lamella's speed and energy. Without knowing the deformation field,

[§]It is noteworthy that air properties, especially ambient pressure, can significantly change the splash threshold in the jet case. Ongoing work is focused on these effects but for the sake of simplicity air properties are here assumed to be fixed and not to affect the splash threshold.

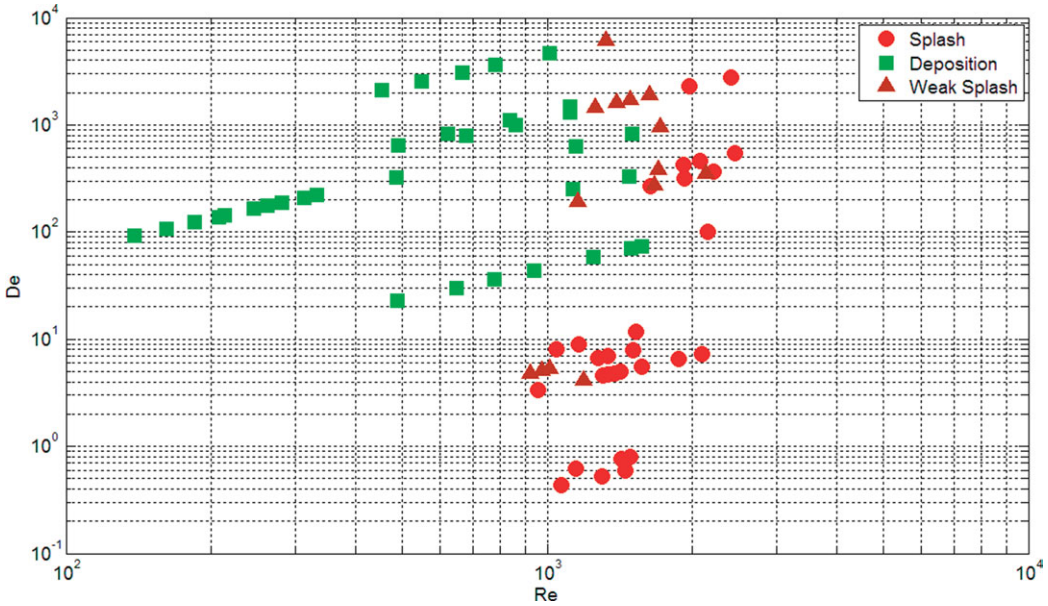

Figure 11. Splash/nonsplash boundary for elastic liquids impacting on the rough surface.

[Color figure can be viewed in the online issue, which is available at wileyonlinelibrary.com.]

the exact effects of elongational properties are not known. One may still make a simple model using some approximations. In the case of the Newtonian jet, the shear viscosity resists splash through its effect on the lamella's thickness growth with time ($h = c_1\sqrt{vt}$). One may similarly account for the effect of extensional viscosity. It was always observed during experiments that the lamella's thickness is much higher for elastic liquids than Newtonian ones (e.g. compare Figures 8A and 9A), which is consistent with previous measurements of the effects of polymer addition on droplet impaction.[32]

We propose that a reasonable approximation for the lamella thickness for an elastic liquid is

$$h_{\text{elastic}}(t) = (1 + cDe^m)\sqrt{vt} \tag{10}$$

In Eq. 10, h_{elastic} is the lamella thickness at time t for the elastic liquid, and c and m are scaling constants that are functions of surface roughness patterns and air properties.

If one uses this correlation for lamella thickness in the jet impact model, the splash threshold criterion can be worked out using the same assumptions made in the Newtonian case. The new criterion will be the following

$$\frac{We.Re^2}{(1 + cDe^m)^2}\left[\frac{1}{6} - \left(\frac{1}{6}\sin^2\alpha + \frac{1 + cDe^m}{Re}\sin\alpha\right)\right]^2 \geq K \tag{11}$$

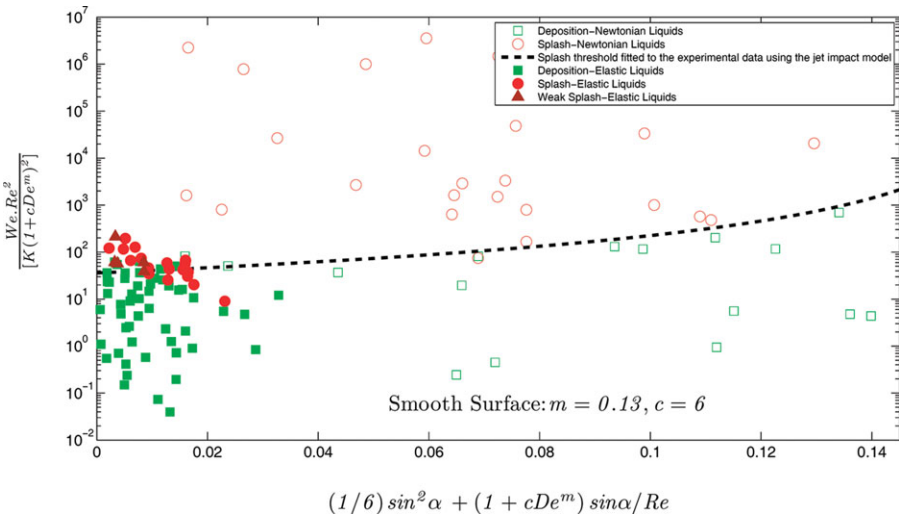

Figure 12. Comparison of experimental data with fitted splash threshold (see text) for both Newtonian[24] and elastic liquids.

Impaction on a smooth surface ($K = 3 \times 10^5$ for Newtonian solutions and $K = 9.2 \times 10^5$ for elastic liquids). [Color figure can be viewed in the online issue, which is available at wileyonlinelibrary.com.]

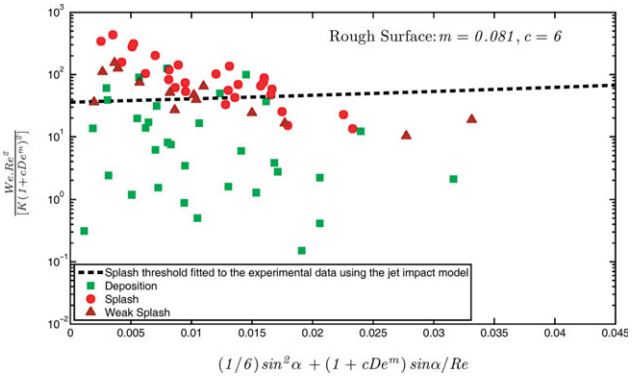

Figure 13. Comparison of elastic liquid splash with semianalytical splash threshold (see text) for rough surface ($K = 6.8 \times 10^5$).

[Color figure can be viewed in the online issue, which is available at wileyonlinelibrary.com.]

Equation 11 is identical in form to Eq. 9 if the Reynolds number in Eq. 9 is replaced by a modified dimensionless group ($\Pi \equiv \frac{Re}{1+cDe^m}$). This new dimensionless variable also has a physical significance; it is approximately the ratio of inertia forces to the sum of the elastic and viscous forces in the lamella.

Figures 12 and 13 show the theoretical splash threshold (Eq. 11) relative to the experimental data for smooth and rough surfaces. The y axis in these graphs is normalized by values of K in each case ($K = 3 \times 10^5$ for Newtonian liquids on the smooth surface; $K = 9.2 \times 10^5$ for elastic liquids on smooth surfaces; and $K = 6.8 \times 10^5$ for elastic liquids on rough surfaces), and also $c = 6$ for both smooth and rough surfaces. The value of m (0.13 for the smooth surface and 0.081 for the rough surface) is selected based on the slope of the separating lines in the corresponding Deborah vs. Reynolds number graphs (i.e., Figures 10 and 11). One interesting result apparent in Figure 12 is that the normalized splash threshold using the new dimensionless

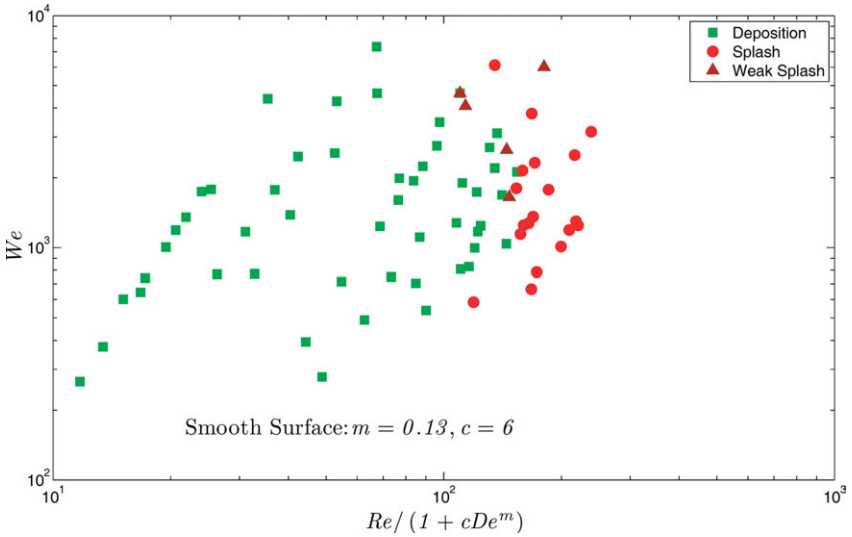

Figure 14. Splash/nonsplash boundary for elastic liquids impacting on the smooth surface.

[Color figure can be viewed in the online issue, which is available at wileyonlinelibrary.com.]

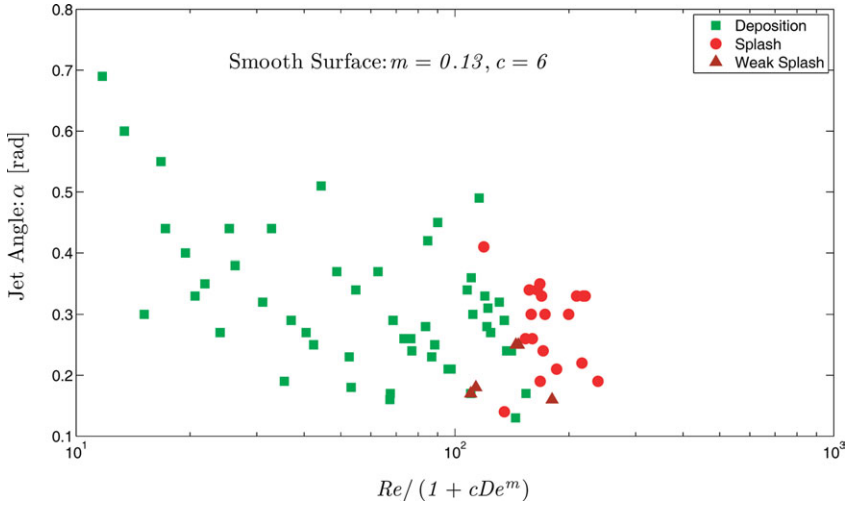

Figure 15. Splash/nonsplash boundary for elastic liquids impacting on the smooth surface.

[Color figure can be viewed in the online issue, which is available at wileyonlinelibrary.com.]

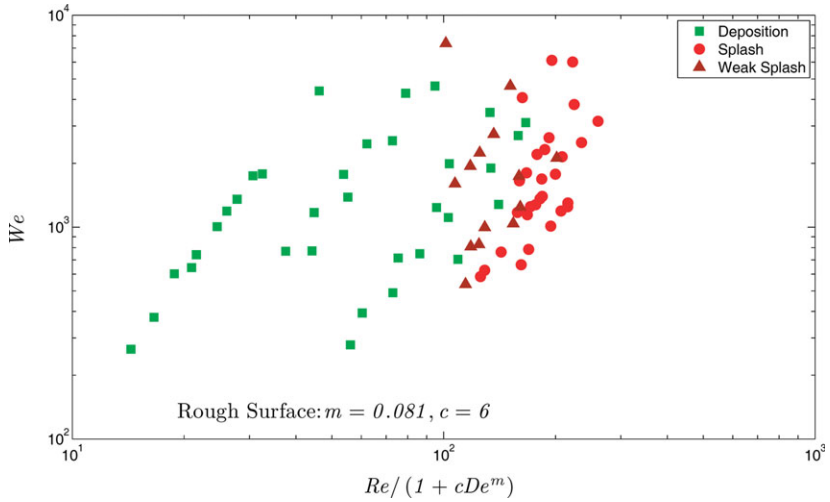

Figure 16. Splash/nonsplash boundary for elastic liquids impacting on the rough surface.

[Color figure can be viewed in the online issue, which is available at wileyonlinelibrary.com.]

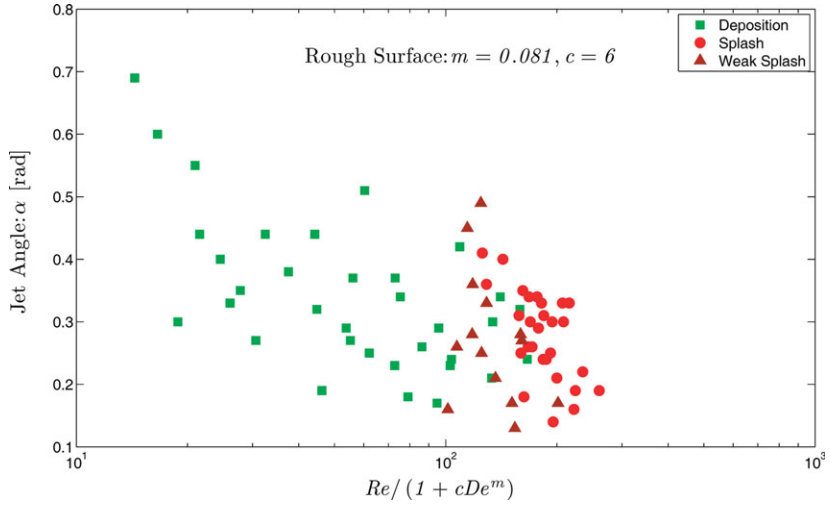

Figure 17. Splash/nonsplash boundary for elastic liquids impacting on the rough surface.

[Color figure can be viewed in the online issue, which is available at wileyonlinelibrary.com.]

group (Π) collapses reasonably the elastic liquid results on the Newtonian data for smooth surface impaction.[¶]

Several other interesting results can be seen from the model:

- For low pathline angles ($\alpha \to 0$) the threshold is mainly a function of $\frac{We \cdot Re^2}{(1+cDe^m)^2}$; its dependence on angle is negligible.
- Keshavarz et al.[24] showed that in the case of Newtonian liquid jet impact, the splash threshold is primarily a function of $We \cdot Re^2$. A simple sensitivity analysis of this function shows that the Reynolds number has a much greater impact on the splash threshold than the Weber number.[24] The same argument holds here for our new splash threshold, for which $\frac{Re}{(1+cDe^m)}$ is more important than the Weber number.

These model predictions are qualitatively verified by plotting splash/deposition in Weber vs. Π and jet pathline angle (α) vs. Π coordinates. Figures 14 and 15 for the smooth surface and Figures 16 and 17 for the rough surface show that the dominant dimensionless group in determining the splash threshold is Π for both smooth and rough surface impact. The effects of Weber number (Figures 14 and 16) and also jet angle (Figures 16 and 17) are smaller than Π for both smooth and rough surface impact. The simple model of jet splash and the experimental results both show that the main controlling parameters for avoiding splash are viscosity (through reduction of Reynolds number) and elasticity of the liquid (through increase of Deborah number).

[¶]There were insufficient data for Newtonian jet impaction on a rough surface to draw conclusions for that case.

Conclusions

Twelve different samples of elastic liquids (PEO solutions) were prepared and tested to study the effects of elasticity on the liquid jet impingement on a high-speed moving surface. The experiments and the results are qualitatively consistent with previous works of both single elastic droplet impaction and Newtonian jet impingement on a moving surface. A simple model, extended from Newtonian data analysis, was used for the elastic liquids and model predictions for small jet pathline angles were verified by experimental observations.

The key findings of this study are:

- Adding elasticity significantly increased the splash threshold relative to a Newtonian liquid of equal viscosity.
- For both smooth and rough surfaces, the most important dimensionless numbers were the Reynolds and Deborah numbers.
- As was also the case for the Newtonian liquid jet impaction, the Weber number and jet pathline angle play only a small role in impaction.

Acknowledgments

This research was sponsored by Kelsan Technologies Corporation and the Natural Sciences and Engineering Research Council of Canada (NSERC).

Notation

D = diameter, m
R = radius, m
V = velocity, $m \cdot s^{-1}$
V_{rel} = relative velocity, $m \cdot s^{-1}$
Re = Reynolds number based on relative velocity
We = Weber number based on relative velocity
α = jet pathline angle in solid surface frame of reference, rad
σ = surface tension, $N \cdot m^{-1}$
ε = roughness height, m
μ = viscosity, Pa·s
ν = kinematic viscosity, $m^2 \cdot s^{-1}$
ρ = density, $kg \cdot m^{-3}$
Wt = weight
C_d = discharge coefficient
m° = mass flow rate, $kg \cdot s^{-1}$
A_n = Nozzle Area, m^2
λ = largest relaxation time, s
De = Deborah number
El = Elasticity number
m = separating line slope
Π = dimensionless number

Literature Cited

1. Li LKB, Dressler DM, Green SI, Davy MH, Eadie DT. Experiments on air-blast atomization of viscoelastic liquids. 1. Quiescent conditions. *J Atomization Sprays*. 2009;19:157–190.
2. Cotter J, Eadie DT, Elvidge D, Hooper N, Robert J, Makowsky T, Liu Y. Top of rail friction control: reductions in fuel and greenhouse gas emissions. Proceedings of the 2005 Conference of the International Heavy Haul Association, Rio de Janeiro, 2005; 327–334.
3. Dressler DM, Li LKB, Green SI, Davy MH, Eadie DT, Newtonian and non-Newtonian spray interaction with a high-speed moving surface. *J Atomization Sprays*. 2009;19:19–39.
4. Li LKB, Green SI, Davy MH, Eadie DT. Air-blast atomization of viscoelastic liquids in a cross-flow. Part 1. Spray penetration and dispersion. *J Atomization Sprays*. 2010;20:697–720.
5. Li LKB, Green SI, Davy MH, Eadie DT. Air-blast atomization of viscoelastic liquids in a cross-flow. Part 2. Droplet velocities. *J Atomization Sprays*. 2010;20:721–735.
6. Rein M. Phenomena of liquid drop impact on solid and liquid surfaces. *Fluid Dynam Res*. 1993;12:61–93.
7. Rioboo R, Marengo M, Tropea C. Time evolution of liquid drop impact onto solid, dry surfaces. *Exp Fluid*. 2002;33:112–124.
8. Yarin AL. Drop impact dynamics: splashing, spreading, receding, bouncing…. *Annu Rev Fluid Mech*. 2006;38:159–192.
9. Deegan RD, Brunet P, Eggers J. Complexities of Splashing, *Nonlinearity*. 2008;21:1–11.
10. Range K, Feuillebois F. Influence of surface roughness on liquid drop impact. *J Colloid Interface Sci*. 1998;203:16–30.
11. Crooks R, Boger D. Influence of fluid elasticity on drops impacting on dry surfaces. *J Rheol*. 2000;44:973–996.
12. Mundo C, Sommerfield M, Tropea C. Droplet-wall collisions: experimental studies of the deformation and breakup process. *Int J Multiphase Flow*. 1995;21:151–173.
13. Povarov OA, Nazarov OI, Ignat'evskaya LA, Nikol'skii AI. Interaction of drops with boundary layer on rotating surface. *J Eng Phys*. 1976;31:1453–1456.
14. Courbin L, Bird JC, Stone HA. Splash and anti-splash: observation and design. *Chaos*. 2006;16:041102.
15. Okawa T, Shiraishi T, Mori T. Effect of impingement angle on the outcome of single drop impact onto a plane water surface. *Exp Fluids*. 2008;44:331–339.
16. Fathi S, Dickens P, Fouchal F. Regimes of droplet train impact on a moving surface in an additive manufacturing process. *J Mater Process Technol*. 2010;210:550–559.
17. Bird JC, Tsai SSH, Stone HA. Inclined to splash: triggering and inhibiting a splash with tangential velocity. *New J Phys*. 2009;11: 1–6.
18. Ruiter JD, Pepper RE, Stone HA. Thickness of the rim of an expanding lamella near the splash threshold. *Phys Fluids*. 2010; 22:1–9.
19. Bergeron V, Bonn D, Martin JY, Vovelle L. Controlling droplet deposition with polymer additives. *Nature*. 2000;405:772–775.
20. Roux DC, Cooper-White JJ, McKinley GH, Tirtaatmadja V. Drop impact of Newtonian and elastic fluid. *Phys Fluids*. 2003;15:S12.
21. Dressler DM. An experimental investigation of Newtonian and non-Newtonian spray interaction with a moving surface. M.A.Sc. Thesis UBC. 2006.
22. Liu X, Lienhard(V) JH. The hydraulic jump in circular liquid impingement and in other thin films, *Exp Fluids*. 1993;15: 108–116.
23. Hlod A, AArts ACT, van de Ven AAF, Peletier MA. Mathematical model of falling of a viscous jet onto a moving surface. *Eur J Appl Math*. 2007;18:659–677.
24. Keshavarz B, Green SI, Davy MH, Eadie DT. Newtonian liquid jet impaction on a high-speed moving surface. *Int J Heat Fluid Flow*. 2011;32:1216–1225.
25. Rodd LE, Scott TP, Cooper-White JJ, McKinley GH. Capillary breakup rheometry of low-viscosity elastic fluids. *Appl Rheol*. 2005;15:12–27.
26. Doi M, Edwards SF. *Theory of Polymer Dynamics*, 1st ed. Oxford University Press, Clarendon, 1988.
27. Lefebvre AW. *Atomization and Sprays*. 1st ed. Hemisphere Publishing Corporation, New York, 1989.
28. Boger DV. Visco-elastic flows through contractions. *Annu Rev Fluid Mech*. 1987;19:157–182.
29. Boger DV, Walters K. Experimental dilemmas in non-Newtonian fluid mechanics and their theoretical resolution. *Korea-Australia Rheol J*. 2000;12:27–38.
30. Rothstein J, McKinley GH. The Axisymmetric contraction-expansion: the role of extensional rheometry on vortex growth dynamics and the enhanced pressure drop. *J non-Newtonian Fluid Mech*. 2001;98:33–63.
31. Cartalos U, Piau JM. Creeping flow regimes of low concentration polymer solutions in thick solvents through an orifice die. *J Non-Newtonian Fluid Mech*. 1992;45:231–285.
32. Cooper-White JJ, Crooks RC, Boger DV. A drop impact study of worm-like viscoelastic surfactant solutions. *Colloids and Surface*. 2002;210:105–123.

Manuscript received Mar. 24, 2011, revision received Nov. 1, 2011, and final revision received Jan. 10, 2012.